3-D Printed Dual-Band Filter Based on Spherical Dual-Mode Cavity

3-D Printed Dual-Band Filter Based on Spherical Dual-Mode Cavity

Yuan Chen, Gang Zhang, Jiasheng Hong, *Fellow, IEEE,* Zhengyu Sun, Jiquan Yang, Wanchun Tang and Chunmei Feng

***Abstract* — A new dual-band bandpass filter (BPF) is designed and fabricated based on a pair of spherical dual-mode resonant cavities using 3-D printing technology. By elaborately introducing three-type metallic posts into each cavity to perturb the degenerated TM_{101} modes in a reasonable way, a dual-band coupling topology is developed in the design, accordingly. Owing to the cross coupling paths in designed topology, two transmission zeros (TZs) are successfully introduced between the passbands, bringing out a high band-to-band isolation. Even more TZs can also be generated by creating additional internal coupling paths to the presented dual-band coupling topology. Besides, the spherical cavity provides higher quality factor and wider stopband, compared to that of square or cylindrical cavity. To validate the design concept, a dual-band BPF prototype operating at 12.0 GHz and 12.5 GHz with respective bandwidths of 120 MHz and 240 MHz is implemented by 3-D printing process. Measured results exhibit a good agreement with simulated ones, showing better than 20 dB return losses and 20 dB dual-band isolation.**

***Index terms*—bandpass filter, dual-mode, dual-band, 3-D printed, higher *Q*, spherical cavity resonators.**

I. INTRODUCTION

Microwave dual-band passband filters (BPFs) are key components of the wireless dual-band communication system. How to attain miniaturization and high performance of them has become one hot topic. To meet this demand, a widely used method to realize the dual-band BPF is the use of dual-mode resonators, due to the fact that the number of resonators required for a given degree of filter can be reduced by half, always resulting in a compact filter configuration. Typically, microstrip BPFs with dual-mode response are attractive, of which each dual-mode resonator can be used as a doubly tuned resonant circuit in simple configurations, e.g., stepped impedance resonators (SIR) [1]-[2] or microstrip ring-resonator [3]-[4]. Specifically, in [1], two single short-stub-loaded folded SIRs are applied to design a high selective dual-band dual-mode microstrip BPF. Without adding any additional perturbation element in [3], a single ring resonator realizes dual passbands response, good in-band matching and outside rejections.

Manuscript received November 27, 2020. This work was supported in part by China Postdoctoral Science Foundation under Grant 2020M682646 and Key R&D Program of Jiangsu Province under Grant BE2018010.

Y. Chen, G. Zhang, Z. Sun, J. Yang, W.Tang and C.Mei are with Jiangsu Key Laboratory of 3D Printing Equipment and Manufacturing, School of Electrical and Automation Engineering, Nanjing Normal University, Nanjing 210046, China. G. Zhang is also with Guangdong Shenglu Telecommunication Tech. Co., Ltd and South China University of Technology. (e-mail: gang_zhang@126.com).

J. S. Hong is with the Department of Electrical, Electronic and Computer Engineering, School of Engineering and Physical Sciences, Heriot-Watt University, Edinburgh EH14 4AS, U.K. (e-mail: j.hong@hw.ac.uk).

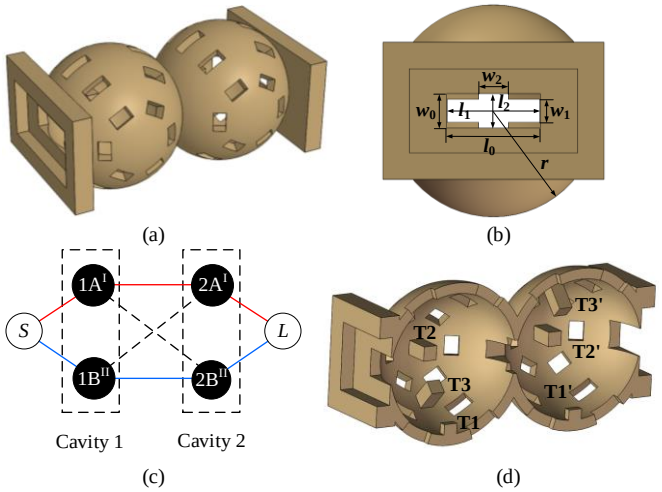

Fig. 1 A geometrical illustration of the dual-band bandpass filter. (a) A 3-D view, (b) a side view of the cross-iris, (c) coupling topology(white nodes: source (S) and load (L); black nodes: resonant modes; solid/dashed lines: direct/cross couplings; red lines: the first-band; bule lines: the second-band), (d) fabrication model in half showing inside structural detail with the metallic posts indicated by T1, T1' and so on.

However, these microstrip resonators have the drawback of low *Q* factor and cannot be applied to high frequency. To solve this problem, cavity dual-band BPF with compact configuration and high *Q* have drawn a growing attention, such as rectangle cavity dual-band BPFs [5]-[6] and dual-band elliptical cavity [7], etc. Compared to above mentioned rectangle and elliptical cavity resonators, spherical cavity resonators have higher *Q* factor. Multiple spherical cavity resonators are cascaded through the coupling slot to achieve desired filtering function [8]-[13]. For instance, a fifth-order spherical cavity BPF is designed in [9] based on an Olympic-shape coupling topology, bringing out an improved high-side out-of-band rejection while the structure lacks compactness. In [10], by etching several slots into spherical resonators, a third-order spherical cavity BPF is presented with a wide spurious-free stopband. Although these BPFs based on spherical cavity resonator have good filtering performance, to the best of our knowledge, there is few report on the design of spherical cavity dual-band BPF.

The primary motivation of this letter is to propose a new and effective design method for dual-band BPF based on high *Q* spherical cavity resonator. By virtue of elaborately perturbing the degenerated TM_{101} modes with three-type metallic posts in two coupled spherical cavity resonators, a dual-mode dual-band cross-coupled topology is developed. For validation, a prototype BPF with operating at 12.0 GHz and 12.5 GHz is ultimately realized with the help of 3-D printing technology, owing to the designed irregular structures. The simulation results coincide well with the measured ones, indicating a nice dual passbands filtering response and band-to-band isolation.

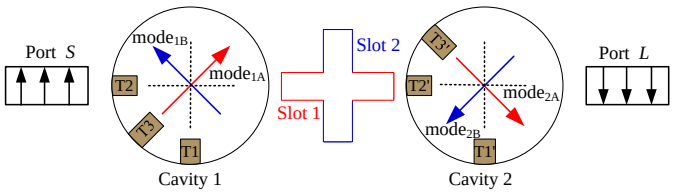

Fig.2 A longitudinal section schematic view of the cavities, their coupling slots and input/output ports with the corresponding *E*-filed directions.

II. Design and Analysis

The configuration of dual-band bandpass filter is shown in Fig. 1. It consists of a pair of hollow spherical cavity resonators loaded with three-type metallic posts into each cavity. The pair of spherical cavities are externally coupled with two input and output waveguide feeds WR-75 through a pair of rectangular apertures, respectively. While they are internal coupled by a pair of cross slots as shown in Fig. 1(b). Besides, it can be observed from Fig.1(d) that a first-type metallic post T1 is arranged at −90 °direction of one cavitiy and the metallic post T1' is arranged at the same direction of the other cavity. Then a pair of metallic posts [T2 and T2'] as second-type ones are arranged at +180 °direction of the two cavities, respectivly. Moreover, two additional metallic posts as third-type ones [T3 and T3'] are placed at +/−135 °directions of both the cavities.

Fig. 2 describes a longitudinal section schematic view of the two designed coupled cavities (cavity 1 and 2), their coupling slots (slot 1 and slot 2) and input/output ports. When the input signal is coupled from input port *S* to cavity 1, both $mode_{1A}$ and $mode_{1B}$ in cavity 1 will be excited with orthogonal *E*-field directions as shown in the figure. Note that the presented *E*-field directions of the two modes are key for dual-band operation and angled with the respect to the dashed lines, which has been investigated to be caused by the loaded post T3. Besides, since the $mode_{1A}$ and $mode_{1B}$ are at low and high resonant frequencies and their *E*-field directions are vertical with each other, there is no coupling between them. Then, through the coupled slots, the signal will be further transmitted to cavity 2, and correspondingly, $mode_{2A}$ and $mode_{2B}$ will be excited in cavity 2 with the orthogonal *E*-field directions, which can be observed from the figure. As the coupling between $mode_{1A}$ and $mode_{2A}$ in the two cavities for the first passband is mainly through the horizontal slot 1, the sign of it can be judged as positive with vector decomposition of *E*-field direction of them. In a similar way, due to that the coupling between $mode_{1B}$ and $mode_{2B}$ in the two cavities for the second passband is mainly through the vertical slot 2, the sign of it can be determined as negative. In addition, as the *E*-field directions of $mode_{1A}$ and $mode_{2B}$ ($mode_{1B}$ and $mode_{2A}$) are opposite with each other, there are negative cross couplings between them, resulting in a pair of TZs for good band-to-band isolation. Finally, the signal is coupled to output port *L* from cavity 2, bringing out the external coupling between $mode_{2A}$ ($mode_{2B}$) and port *L*.

Based on the above anlysis, Fig. 1(c) describes the according developed dual-band coupling topology, where the superscripts I and II represent the first and second passbands, respectively. As observed, the first passband is dominated by the corresponding $mode_{1A}$ and $mode_{2A}$ while the second one is

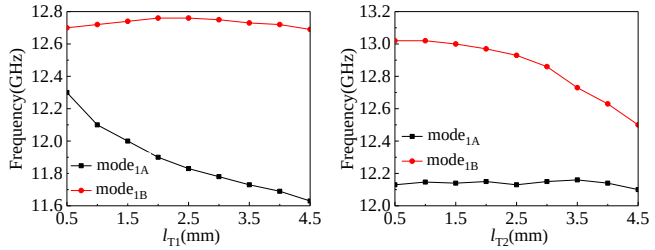

Fig.3 Resonant frequencies of $mode_A$ and $mode_B$ under different metallic posts. (a) lengths l_{T1} (l_{T2}=3.5mm), (b) lengths l_{T2} (l_{T1}=0.5mm).

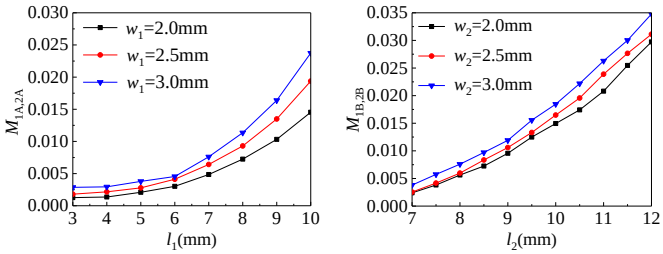

Fig.4 Internal coupling coefficients under (a) different coupling slot lengths l_1 and various w_1, (b) different coupling slot lengths l_2 and various w_2.

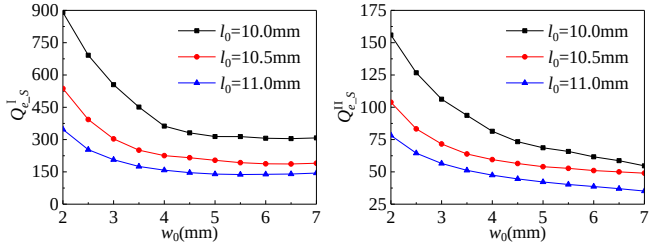

Fig.5 External quality factor of each passband ($Q^i_{e\_S}$) varies with w_0. (a) the first-band, (b) the second-band.

determined by the corresponding $mode_{1B}$ and $mode_{2B}$ from the two cavities. On the basis of the above concept, a dual-band spherical cavity BPF centered at 12.0 GHz and 12.5 GHz with the respective bandwidths of 120 MHz and 240 MHz is designed for an example.The needed coupling coefficients *M* and external quality factors Q_e for the circuit are obtained by utilizing the well known optimization synthesis process provided in [14] as $M_{1A,2A}$=0.00481, $M_{1B,2B}$= -0.00652, and $Q^I_{e\_S} = Q^I_{e\_L}$= 230.0, $Q^{II}_{e\_S}= Q^{II}_{e\_L}$=61.6. Based on the required resonant frequencies of the two passbands, the physical dimensions of the cavities and metallic posts can be readily determined with the help of spherical cavity model theory in [15] and parameter studies of the design parameters of the metallic posts as shown in Fig.3. Besides, the desired internal couplings between the spherical cavity 1 and 2 and external quality factor ($Q^i_{e\_S}$) can be extracted from the following,

$$\left|M_{1j,2j}\right| = \frac{f_{1j}^2 - f_{2j}^2}{f_{1j}^2 + f_{2j}^2},\ j=\text{A,B};\quad Q^i_{e\_s} = \pi f_i \cdot \tau_{S_{11}}(f_i)/2,\ i=\text{I, II} \quad (1)$$

Fig. 4 shows the extracted main internal coupling coefficients versus varied coupling slot lengths and widths. As observed, these required internal coupling coefficients could be realized by determining a proper coupling slot length and width. Fig. 5 illustrates the extracted curves of $Q^I_{e\_S}$ ($Q^{II}_{e\_S}$) from group delay

This article has been accepted for publication in a future issue of this journal, but has not been fully edited. Content may change prior to final publication. Citation information: DOI 10.1109/LMWC.2021.3080430, IEEE Microwave and Wireless Components Letters

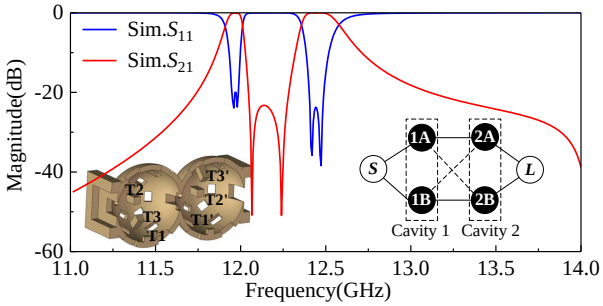

Fig.6 Simulated results of the presented dual-band dual-mode BPF.

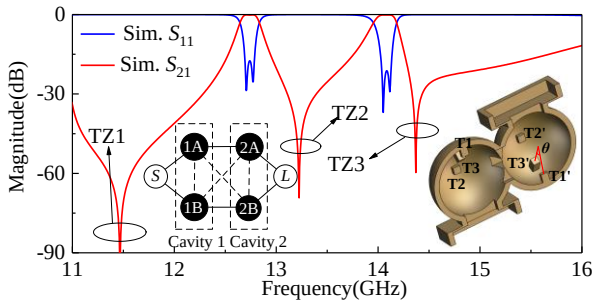

Fig.7 Simulated results of the improved dual-band filter with three TZs (r=10, l_0 = 10.1, w_0 = 4, l_1 = 9.8, w_1 = 2.2, l_2 = 9.4, w_2 = 2.2, l_{T1}= $l_{T1'}$= 2.4, l_{T2}= $l_{T2'}$= 2, l_{T3}= $l_{T3'}$= 5 (all units: mm), θ =48° .

TABLE I
COMPARISON OF THREE TYPES OF DUAL-MODE CAVITY RESONATOR

Shape	Rectangle	Cylindrical	Spherical
Dimension(mm)	16×16×17	10(R) 16(H)	10(R)
Volume(mm^3)	4352	5024	4187
Dominant mode	TE_{011}/TE_{101}	TE_{111}/TM_{011}	TM_{101}
Q_u@13GHz	8843	10950	12379
First spurious mode	TM_{110} (16GHz)	TM_{011} (15GHz)	TM_{2m1} (18GHz)

versus the input apertures width w_0 with length l_0 as a variable. It can be found that when w_0 increases, $Q^{I}_{e\_s}$ ($Q^{II}_{e\_s}$) decreases while the same case can been found for l_0. The above graphs could be used to help design the proposed dual-band BPF.

EM-simulations of the BPF were performed using the high frequency structure simulation (HFSS). Thereinto, copper with an electrical conductivity of 5.8×10^7 S/m is used for the cavity boundaries in the simulation. Fig.6 exhbits the simulated results of the presented dual-band BPF with nice operation performance. In addition, Table I shows three types of dual-mode cavity resonators comparision in terms of factor Q_u, as well as suprious suppression performance. It demonstrates advantages of using spherical cavity over the others. The spherical dual-mode resonator offers the highest Q_u at the same resonant frequency of 13 GHz and the first spurious resonance at 18 GHz, which is much further than that of the others (at 16 GHz and 15 GHz for dual-mode rectangle and cylindrical resonators, respectively). Moreover, spherical cavity has much compact size compared with others.

On the other hand, in order to better verify the flexibility of the proposed method, an extended discussion is worth being given here. Based on our design concept, an improved topology can also be developed by creating additional internal coupling

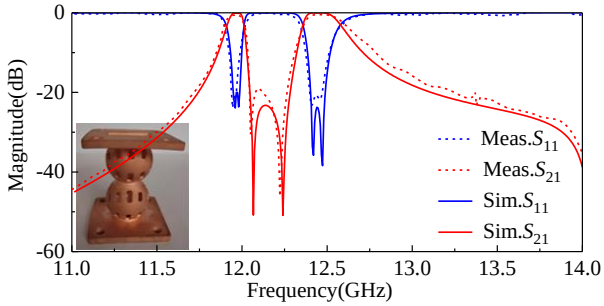

Fig.8 Measured and simulated results of the presented dual-band BPF in Fig.1.

from the previous topology, as described in the inset of Fig.7. In line with the topology, another new dual-band filter can be further proposed with more TZs by adjusting the angle of posts T3 and T3' and the position of ports from the previous design, of which bisection are shown in the figure. Its corresponding simulated results with nice improvement can be observed in the Fig.7, well validating the flexibility of our proposal.

III. IMPLEMENTATION, RESULTS AND DISCUSSION

To verify the above design concept, a prototype dual-band BPF in Fig.1 is finally realized by taking full advatages of SLS 3D-printing technology with the PA12 (nylon material) as a whole structure and then metalized with a 10-μm thick copper layer. It should be noted that this 10-μm thick copper has been taken into consideration in the simulation. The employed metallization method is based on traditional electroless copper and electroplating procedures. The photo of the final fabricated dual-band BPF is shown in the inset of Fig. 8. Its final dimensions referring to Fig.1 is determined as: r =10, l_0 = 10.6, w_0 = 3.9, l_1 = 10.4, l_2 = 9.4, w_1 = 2.5, w_2 = 3.4, l_{T1}= $l_{T1'}$=3.5, l_{T2}= $l_{T2'}$=0.5, l_{T3}= $l_{T3'}$= 3.6 (all units: mm). The posts sizes are all 2 mm × 2 mm. The effective size is 42 mm × 38 mm ($1.707\lambda_g \times 1.545\lambda_g$), where λ_g denotes the guided wavelength at the center frequency of the whole virtual passband.

Fig. 8 shows the simulated and measured S-parameter results, which coincide well with each other. Observed that the dual-band BPF exhibits that the center frequencies of two passbands are 12.0 GHz and 12.49 GHz with 3-dB bandwidths of 120 MHz and 240 MHz, respectively. The measured minimum in-band ILs are around 0.6 dB and 0.45 dB while the passband RLs are all about 20 dB. Moreover, two TZs appear at about 12.06 GHz and 12.25 GHz, respectively, bringing out good band-to-band isolation.

IV. CONCLUSION

This letter has presented a new and effective design method for dual-band filter based on dual-mode spherical cavity. The analysis and design principle have been throughly described. Compared to conventional cavity resonators operating at the same resonant frequency, the spherical dual-mode resonator offers much higher Q_u and smaller dimension. Good agreement between the measured and simulated results demonstrates the feasibility of our design method and 3D printing technology, which shows great potential of the spherical cavity BPF for multichannel communication applications.

REFERENCES

[1]. W. Chen, Y. Zhao and X. Zhou, "Compact and high selectivity dual-band dual-mode microstrip BPF with folded SIR," *IEEE MTT-S Int. Microw. Workshop*., Nanjing, China, Sept. 2012，pp. 1-3.

[2]. H. Liu et al., "Compact and high selectivity tri-band bandpass filter using multimode stepped-impedance resonator," *IEEE Microw. Wireless Compon. Lett.*, vol. 23, no. 10, pp. 536-538, Oct. 2013.

[3]. S. Sun, "A dual-band bandpass filter using a single dual-mode ring resonator," *IEEE Microw. Wireless Compon. Lett.*, vol. 21, no. 6, pp. 298-300, Jun. 2011.

[4]. A. Ebrahimi, W. Withayachumnankul, S. F. Al-Sarawi and D. Abbott, "Compact dual-mode wideband filter based on complementary split-ring resonator," *IEEE Microw. Wireless Compon. Lett.*, vol. 24, no. 3, pp. 152-154, Mar. 2014.

[5]. Z. C. Guo, L. Zhu, S. W. Wong, "Modular synthesis of waveguide bandpass filters using dual-mode resonators," *IEEE Trans. Microw. Theory Techn*., vol. 68, no. 5, pp. 1660-1667, May. 2020.

[6]. Z. Guo, S. Wong and L. Zhu, "Triple-passband cavity filters with high selectivity under operation of triple modes," *IEEE Trans. Compon., Packag., Manuf. Technol*., vol. 9, no. 7, pp. 1337-1344, Jul. 2019.

[7]. L. Zhu, R. R. Mansour and M. Yu, "Quasi-elliptic waveguide dual-band bandpass filters," *IEEE Trans. Microw. Theory Techn.*, vol. 67, no. 12, pp. 5029-5037, Dec. 2019.

[8]. J. Li, C. Guo, L. Mao and J. Xu, "3D printed bandpass filters using compact high-*Q* hemispherical resonators with improved out-of-band rejection," *IEEE Electron Lett*, vol. 53, no. 6, pp. 413-415, Mar. 2017.

[9]. J. Li, G. Huang and T. Yuan, "Monolithic 3-D printed spherical resonator based Olympic-topology bandpass filters," *IEEE Int. Sym. Antennas. Propag*., Boston, America, May. 2018, pp. 1441-1442.

[10]. F. Zhang, S. F. Gao, J. Li, Y. Yu, C. Guo, "3-D printed slotted spherical resonator bandpass filters with spurious suppression," *IEEE Access*., vol. 7, pp. 128026-128034, Sep. 2019.

[11]. C. Guo, X. B. Shang, J. Lin, and F. Zhang, "A lightweight 3-D printed X-band waveguide filter based on spherical dual-mode resonators," *IEEE Microw. Wireless Compon. Lett.*, vol. 26, no. 8, pp. 568-570, Aug. 2016.

[12]. J. Li, C. Guo, L. Mao, J. Xiang, G. Huang and T. Yuan, "Monolithically 3-D printed hemispherical resonator waveguide filters with improved out-of-band rejections," *IEEE Access*, vol. 6, pp. 57030-57048, 2018.

[13]. J. Li, K. Hong and T. Yuan, "Slotted hemispherical resonators for 3-D printed waveguide filters with extended spurious-free stopbands," *IEEE Access*, vol. 7, pp. 130221-130235, 2019.

[14]. J. S. Hong and M. J. Lancaster, "Microstrip filters for RF/microwave applications." 2nd ed. 2001, New York: Wiley.

[15]. Lai Sheng-Li and Lin Wei-Gan, "A five mode single spherical cavity microwave filter," *IEEE MTT-S Microw. Sym. Dig*., Albuquerque, NM, USA, 1992, vol.2, pp. 909-912.